JCI The Journal of Clinical Investigation

Inhibition of GSK3β-mediated BACE1 expression reduces Alzheimer-associated phenotypes

Philip T.T. Ly, Yili Wu, Haiyan Zou, Ruitao Wang, Weihui Zhou, Ayae Kinoshita, Mingming Zhang, Yi Yang, Fang Cai, James Woodgett, Weihong Song

J Clin Invest. 2013;123(1):224-235. https://doi.org/10.1172/JCI64516.

Research Article **Neuroscience**

Deposition of amyloid β protein (Aβ) to form neuritic plaques in the brain is the pathological hallmark of Alzheimer's disease (AD). Aβ is generated from sequential cleavages of the β-amyloid precursor protein (APP) by the β- and γ-secretases, and β-site APP-cleaving enzyme 1 (BACE1) is the β-secretase essential for Aβ generation. Previous studies have indicated that glycogen synthase kinase 3 (GSK3) may play a role in APP processing by modulating γ-secretase activity, thereby facilitating Aβ production. There are two highly conserved isoforms of GSK3: GSK3α and GSK3β. We now report that specific inhibition of GSK3β, but not GSK3α, reduced BACE1-mediated cleavage of APP and Aβ production by decreasing *BACE1* gene transcription and expression. The regulation of *BACE1* gene expression by GSK3β was dependent on NF-κB signaling. Inhibition of GSK3 signaling markedly reduced Aβ deposition and neuritic plaque formation, and rescued memory deficits in the double transgenic AD model mice. These data provide evidence for regulation of BACE1 expression and AD pathogenesis by GSK3β and that inhibition of GSK3 signaling can reduce Aβ neuropathology and alleviate memory deficits in AD model mice. Our study suggests that interventions that specifically target the β-isoform of GSK3 may be a safe and effective approach for treating AD.

Inhibition of GSK3β-mediated BACE1 expression reduces Alzheimer-associated phenotypes

Philip T.T. Ly,[1] Yili Wu,[1,2] Haiyan Zou,[1] Ruitao Wang,[1] Weihui Zhou,[2] Ayae Kinoshita,[3] Mingming Zhang,[1] Yi Yang,[1] Fang Cai,[1] James Woodgett,[4] and Weihong Song[1,2]

[1]Townsend Family Laboratories, Department of Psychiatry, Brain Research Center, Graduate Program in Neuroscience, The University of British Columbia, Vancouver, British Columbia, Canada. [2]Ministry of Education Key Laboratory of Child Development and Disorders, and Chongqing City Key Laboratory of Translational Medical Research in Cognitive Development and Learning and Memory Disorders, Children's Hospital of Chongqing Medical University, Chongqing, China. [3]School of Health Sciences, Faculty of Medicine, Kyoto University, Kyoto, Japan. [4]Samuel Lunenfeld Research Institute, Toronto, Ontario, Canada.

Deposition of amyloid β protein (Aβ) to form neuritic plaques in the brain is the pathological hallmark of Alzheimer's disease (AD). Aβ is generated from sequential cleavages of the β-amyloid precursor protein (APP) by the β- and γ-secretases, and β-site APP-cleaving enzyme 1 (BACE1) is the β-secretase essential for Aβ generation. Previous studies have indicated that glycogen synthase kinase 3 (GSK3) may play a role in APP processing by modulating γ-secretase activity, thereby facilitating Aβ production. There are two highly conserved isoforms of GSK3: GSK3α and GSK3β. We now report that specific inhibition of GSK3β, but not GSK3α, reduced BACE1-mediated cleavage of APP and Aβ production by decreasing *BACE1* gene transcription and expression. The regulation of *BACE1* gene expression by GSK3β was dependent on NF-κB signaling. Inhibition of GSK3 signaling markedly reduced Aβ deposition and neuritic plaque formation, and rescued memory deficits in the double transgenic AD model mice. These data provide evidence for regulation of BACE1 expression and AD pathogenesis by GSK3β and that inhibition of GSK3 signaling can reduce Aβ neuropathology and alleviate memory deficits in AD model mice. Our study suggests that interventions that specifically target the β-isoform of GSK3 may be a safe and effective approach for treating AD.

Introduction

Alzheimer's disease (AD) is the most common neurodegenerative disorder leading to dementia. The characteristic neuropathological features of AD include neuritic plaques, neurofibrillary tangles, and neuronal loss. Amyloid β protein (Aβ), the central component of neuritic plaques, is produced from sequential endoproteolytic cleavages of the type 1 transmembrane glycoprotein β-amyloid precursor protein (APP) by β-secretase and γ-secretase. Proteolytic processing of APP at the β site is essential for generating Aβ, and β-site APP-cleaving enzyme 1 (BACE1) is the β-secretase in vivo (1–4). BACE1 cleaves APP at two β-sites, Asp+1 and Glu+11 of the Aβ domain, to generate C99 and C89 fragment, respectively (5). Subsequently, γ-secretase cleaves C99 within its transmembrane domain to release Aβ and APP C-terminal fragment γ (CTFγ). In addition to APP, BACE1 substrates also include other proteins: LRP (6), APLP1 (7), APLP2 (8), ST6Gal I (9), and PSGL-1 (10).

BACE1 expression is tightly regulated at the level of transcription (5, 11, 12) and translation (13–16). It was reported that a G/C polymorphism in exon 5 of the *BACE1* gene might be associated with some sporadic cases of AD (17–19). Although genetic analyses from our and other laboratories have failed to uncover any mutation in the *BACE1* coding sequence or any disease-associated SNP in its promoter region in AD patients (20–22), increased β-secretase levels and activity have been reported in AD (23–27). BACE1 levels were elevated in neurons around plaques (28). *BACE1* mRNA levels tended to increase as miR-107 levels decreased in the progression of AD (29). We reported that hypoxia, a common vascular component among AD risk factors, increased BACE1 expression, resulting in both increased Aβ deposition and memory deficits in AD transgenic mice (30). Recently we found that both NF-κB and BACE1 levels were increased in sporadic AD patients, and NF-κB facilitated *BACE1* gene expression and APP processing (27). Thus, increased BACE1 expression by NF-κB signaling in the brain could be one of the mechanisms underlying AD development (27). Together, these studies indicate that BACE1 dysregulation plays an important role in AD pathogenesis.

BACE1 has been considered as one of the major targets for AD drug development. *Bace1*-knockout mice have abolished Aβ generation (31–33). Suppression of BACE1 by RNA interference reduced APP processing and Aβ production in primary cortical neurons derived from both wild-type and Swedish APP mutant transgenic mice (34), and disruption of the *Bace1* gene rescued memory deficits and cholinergic dysfunction in Swedish APP mice (35). Oral administration of a potent and selective BACE1 inhibitor decreased β-cleavage and Aβ production in APP transgenic mice in vivo (36). *Bace1*-KO mice were reported to display hypomyelination of peripheral nerves and aberrant axonal segregation (37, 38), suggesting that inhibiting β-secretase may have unwanted collateral effects. However, even a partial reduction in BACE1 can have dramatically beneficial effects on AD pathology (39), suggesting that therapeutic inhibition of BACE1 is a valid therapeutic target for AD treatment.

Authorship note: Philip T.T. Ly and Yili Wu contributed equally to this work.
Conflict of interest: The authors have declared that no conflict of interest exists.
Citation for this article: *J Clin Invest.* 2013;123(1):224–235. doi:10.1172/JCI64516.

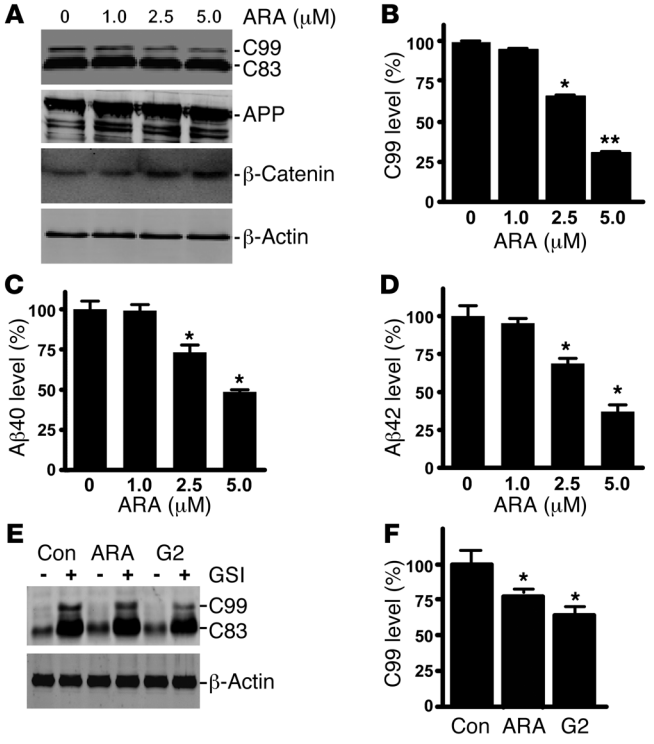

Figure 1

Specific inhibition of GSK3 reduces BACE1 cleavage of APP. (**A**) Swedish mutant APP stable cell line 20E2 was cultured and treated with ARA for 24 hours, and cell lysates subjected to Western blot analysis. Full-length APP and the APP CTFs were detected with C20 antibody. β-Catenin was detected by anti–β-catenin antibody. β-Actin was detected by anti-actin antibody AC-15 as the internal control. (**B**) Quantification of APP C99 generation in 20E2 cells. ARA treatment significantly increased β-catenin levels in a dose-dependent manner, while APP C99 production decreased with increasing ARA dosage. $n = 6$; $^*P < 0.05$ and $^{**}P < 0.01$, ANOVA. Aβ ELISA detection of Aβ40 (**C**) and Aβ42 (**D**) in conditioned medium from 20E2 cells treated with ARA for 24 hours. ARA treatment reduced Aβ levels in the conditioned medium in a dose-dependent manner. The values are expressed as mean ± SEM. $n = 4$; $^*P < 0.05$, ANOVA. (**E**) γ-Secretase activity in 20E2 cells was inhibited by the pharmacological inhibitor L685,458 (GSI). Co-treatment with specific GSK3 inhibitors ARA and G2 reduced C99. Con, control. (**F**) Quantification of C99 levels. $n = 6$; $^*P < 0.05$, ANOVA.

Glycogen synthase kinase 3 (GSK3) is a proline-directed serine/threonine protein kinase originally identified as playing an important role in glycogen metabolism. Since its discovery, many studies have shown that GSK3 has pleiotropic functions, including embryonic development, gene transcription, and neuronal cell function (40). In mammals, two GSK3 isoforms are encoded by distinct genes: *GSK3A* produces a 51-kDa GSK3α protein and *GSK3B* a 47-kDa GSK3β protein (41). These two isoforms are highly homologous, sharing greater than 95% amino acid identity in the catalytic domains. Although both isoforms are ubiquitously expressed, the β isoform is expressed at higher levels in neuronal tissues (42).

GSK3 activity is regulated at several levels. Phosphorylation of Tyr279/Tyr216 on GSK3α/β is important for enzymatic activity (43). Inactivation of GSK3 can be achieved through phosphorylation of Ser21/Ser9 residues within the N-terminal domain on GSK3α/β, respectively. Stimulation of tissues by insulin and growth factors activates the PI3K/PKB/Akt signal transduction cascade, leading to phosphorylation of these inhibitory serine residues (44, 45). GSK3 is also regulated upon interaction of the Wnt ligand and its receptor Frizzled and co-receptor LRP5/6. This interaction releases GSK3 from a multi-protein complex formed by β-catenin, axin, and adenomatous polyposis coli (APC) (46, 47), which prevents GSK3-mediated β-catenin degradation and induces β-catenin–dependent gene transcription.

Dysregulation of GSK3 activity has been implicated in AD. Increased GSK3β activity was found in postmortem AD brains (48). GSK3β has been found to phosphorylate the tau protein on various conserved sites and contribute to tau hyperphosphorylation and neurofibrillary tangle formation (49, 50). GSK3α was reported to regulate Aβ production by positively modulating the γ-secretase complex (51), although this finding has recently been challenged (52). Inhibition of GSK3 activity with the commonly known GSK3 inhibitors LiCl and valproic acid in cell culture (53) and animal models of AD decreased Aβ production (51, 54). Although LiCl and valproic acid are known to inhibit GSK3 activity, these compounds also activate a plethora of signaling cascades that could differentially regulate APP processing independent of GSK3 (55–58).

In this study, we examined the effects of GSK3β-specific inhibition on AD neuropathology and behavioral deficits and identified its underlying mechanism. We found that specific inhibition of GSK3β, but not GSK3α, reduced BACE1-mediated cleavage of APP. Treatment with the GSK3 inhibitor AR-A014418 (ARA) reduced neuritic plaque formation and alleviated memory deficits in AD transgenic model mice. Furthermore, we found that GSK3β regulated *BACE1* transcription via NF-κB signaling. Our work provides evidence that specific inhibition of GSK3β may be an effective therapeutic approach for treating AD.

Results

Regulation of β-secretase cleavage of APP and Aβ production by GSK3 signaling. Previous studies showed that LiCl and valproic acid modulated GSK3 signaling and reduced Aβ production (51, 54). However, the underlying mechanism is not well defined, and these compounds also have many confounding GSK3-independent effects. To examine the specific effect of GSK3 signaling on APP processing, we applied ARA, a highly selective and potent inhibitor of GSK3, to 20E2 cells, a stable cell line expressing human Swedish mutant APP (5). ARA at 1, 2.5, and 5 μM significantly decreased the levels of the β-secretase cleavage product APP C99 to 95.7% ± 1.6%, 66.4% ± 0.7%, and 31.3% ± 0.4%, respectively ($P < 0.001$ by 1-way ANOVA) (Figure 1A and B). The treatment had no significant effect on APP expression (Figure 1A). The Aβ ELISA was performed to assess the levels of Aβ40 and Aβ42 in the conditioned media of 20E2 cells. ARA markedly reduced Aβ

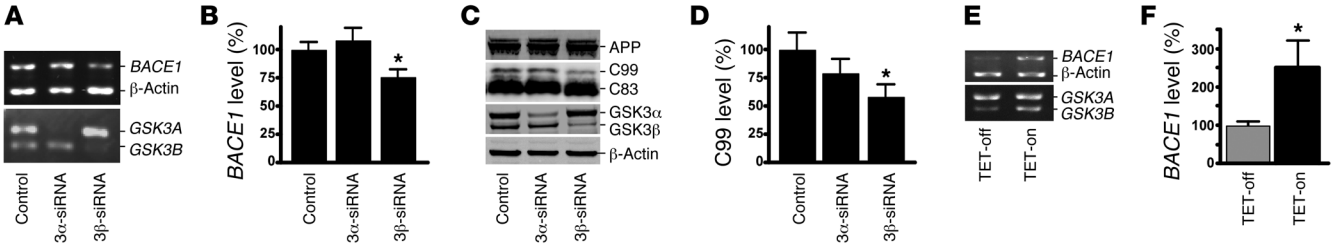

Figure 2

GSK3β, but not GSK3α, regulates *BACE1* gene expression and APP processing. (**A**) SH-SY5Y human neuroblastoma cells were transfected with scrambled GSK3α or GSK3β isoform–specific siRNA. RNA was extracted, and semiquantitative RT-PCR was performed to measure endogenous human *BACE1*, *GSK3A*, *GSK3B*, and β-actin mRNA levels with specific primers recognizing the coding sequence of each gene. PCR products after 28 cycles were analyzed on 1.2% agarose gel. (**B**) Endogenous *BACE1* mRNA was significantly reduced with GSK3β, but not GSK3α, isoform–specific knockdown. The values are expressed as mean ± SEM. $n = 3$; $^*P < 0.05$, Student's *t* test. (**C**) 20E2 cells were transfected with scrambled or GSK3α, or GSK3β isoform–specific siRNA while cotreated with L685,458 to block γ-secretase activity. Full-length APP and CTF fragments were detected with C20 antibody. GSK3α and GSK3β were detected using a monoclonal GSK3α/β antibody. GSK3α and GSK3β isoforms were selectively reduced by the isoform-specific siRNA. β-Actin served as an internal control and was detected using a monoclonal anti–β-actin antibody, AC-15. (**D**) GSK3β-specific knockdown significantly reduced C99 levels. GSK3α-specific knockdown did not have any significant effect. The values are expressed as mean ± SEM. $n = 4$; $^*P < 0.05$, Student's *t* test. (**E**) Tetracycline-regulated SHSY5Y cells were induced to express constitutively active S9A-GSK3β. Endogenous human *BACE1* mRNA levels were assessed as described above. Tetracyline-induced S9A-GSK3β significantly increased BACE1 expression. (**F**) Quantification of the endogenous *BACE1* mRNA level. Values are expressed as mean ± SEM. $n = 4$; $^*P < 0.05$, Student's *t* test.

generation in a dose-dependent manner. Aβ40 was decreased to 99.2% ± 3.8%, 73.2% ± 4.6%, and 48.7% ± 1.3% with 1, 2.5, and 5 μM of ARA treatment, respectively ($P < 0.05$) (Figure 1C); and Aβ42 was reduced to 99.2% ± 3.1%, 73.2% ± 3.5%, and 48.7% ± 4.5% with 1, 2.5 and 5 μM of ARA treatment, respectively ($P < 0.01$ by 1-way ANOVA) (Figure 1D). As expected, inhibition of GSK3 stabilized β-catenin (Figure 1A), and ARA treatment resulted in a significant increase in β-catenin levels to 152.7% ± 11.1%, 221.3% ± 17.0%, and 233.7% ± 25.0% with 1, 2.5, and 5 μM, respectively ($P < 0.05$). These data indicate that specifically inhibiting GSK3 reduced BACE1-mediated APP processing and C99 and Aβ production.

To further examine the effect of GSK3 on β-secretase cleavage of APP and Aβ production, we pharmacologically blocked γ-secretase activity with the γ-secretase–specific inhibitor L658,458 in 20E2 cells while co-treating with the GSK3 inhibitor ARA and G2. G2 is another structurally distinct GSK3 inhibitor, with an IC_{50} of 304 nM (59). As expected, γ-secretase inhibition resulted in markedly increased generation of the APP CTFs C83 and C99 (Figure 1E). Addition of ARA or G2 reduced C99 levels to 78.2% ± 1.1% and 63.9% ± 6.6% (Figure 1, E and F). ARA treatment had no significant effect on Notch cleavage (Supplemental Figure 1B; supplemental material available online with this article; doi:10.1172/JCI64516DS1). These data demonstrated that specific inhibition of GSK3 reduced β-secretase cleavage of APP to generate C99 and Aβ production in cells.

GSK3β but not GSK3α regulates BACE1 gene expression and BACE1-mediated APP processing. Our study has shown that GSK3 regulated β-secretase processing of APP, an essential step for Aβ generation. Since BACE1 is the β-secretase in vivo, we first examined whether GSK3 affects *BACE1* gene expression. GSK3 has two highly homologous isoforms, GSK3α and GSK3β. We used RNA interference to specifically knock down the expression of GSK3α or GSK3β isoforms in human neuroblastoma SH-SY5Y cells to determine whether both isoforms or one of the isoforms play a major role in regulating *BACE1* gene expression. Specific knockdown of GSK3β expression by the siRNA significantly reduced *BACE1* mRNA levels

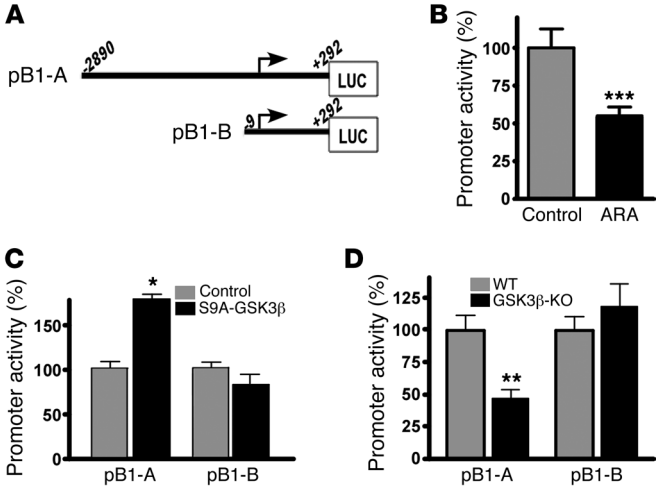

Figure 3

GSK3β regulates *BACE1* promoter activation. (**A**) Schematic of the 3.3-kb (pB1-A) and 300-bp (pB1-B) human *BACE1* promoter/luciferase construct. (**B**) The 3.5-kb human *BACE1* promoter was transfected into N2a cells and treated with 5 μM ARA. GSK3 inhibition with ARA treatment resulted in a significant decrease in luciferase activity. (**C**) N2a cells were co-transfected with either promoter constructs and S9A-GSK3β or a vector control. S9A-GSK3β significantly increased the luciferase activity of the 3.3-kb *BACE1* promoter construct but did not have any effect on the 300-bp promoter construct. (**D**) pB1-A or pB1-B constructs were transfected into *Gsk3b*-KO MEFs. pB1-A had significantly reduced promoter activity. All promoter data shown represent an average of at least 4 independent experiments, with each condition performed in triplicate. Values are expressed as mean ± SEM. $n = 4$; $^*P < 0.05$, $^{**}P < 0.01$, $^{***}P < 0.005$, Student's *t* test.

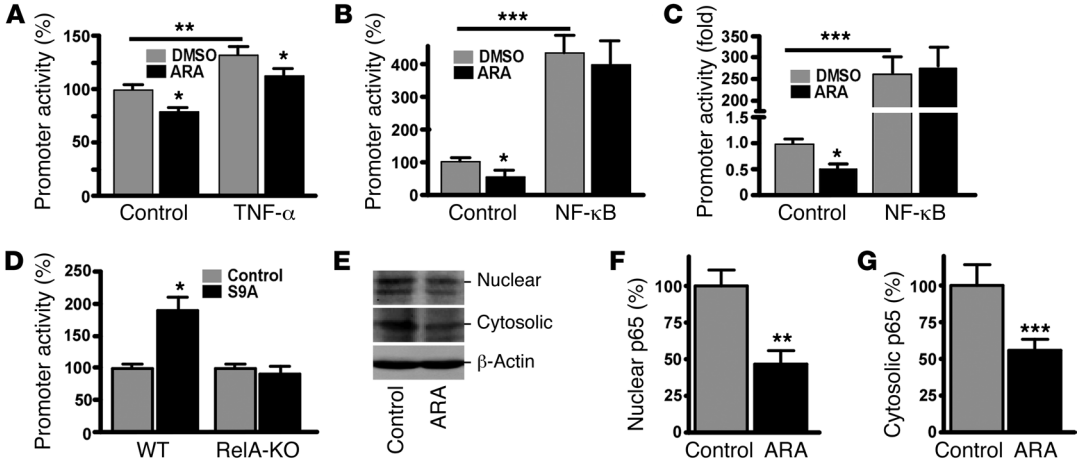

Figure 4

GSK3β regulation of *BACE1* transcription is dependent on NF-κB p65 expression. (**A**) pBACE1-4NF-κB plasmid contains the 4 NF-κB *cis*-elements from the human *BACE1* promoter upstream of the firefly luciferase reporter gene. N2a cells were co-transfected with pBACE1-4NF-κB and pCMV-RLuc. Transfected cells were treated with vehicle solution (control) or 10 ng/ml TNF-α with/without 5 μM ARA for 24 hours. (**B**) N2a cells were co-transfected with pBACE1-4NF-κB plasmid and pMTF-p65 or a vector control. Transfected cells were then treated with a vehicle solution or 5 μM ARA for 24 hours. (**C**) pNF-κB-Luc was co-transfected with pMTF-p65 or a vector control and treated with a vehicle solution or 5 μM ARA for 24 hours. *Renilla* luciferase was used to normalize for transfection efficiency. Values are expressed as mean ± SEM. $n = 4$; $^{*}P < 0.05$, $^{**}P < 0.01$, $^{***}P < 0.001$, Student's *t* test. (**D**) Wild-type MEFs and RelA-KO MEFs which are dysfunctional for NF-κB activity, were co-transfected with a 3.5-kb human *BACE1* promoter and S9A-GSK3β or a control vector. S9A-GSK3β overexpression in MEFs. significantly increased luciferase activity ($^{*}P < 0.05$, Student's *t* test), whereas RelA-KO MEFs did not have any significant effect. Luciferase activity is indicative of *BACE1* promoter activity. All promoter data shown represent an average of at least 4 independent experiments, with each condition performed in triplicate. (**E**) N2a cells were treated with 5 μM ARA for 24 hours, followed by cell fractionation. Cytosolic and nuclear fractions were subjected to SDS-PAGE. ARA treatment significantly reduced NF-κB p65 levels in the (**F**) nuclear fraction ($n = 6$; $^{**}P < 0.001$, Student's *t* test) and (**G**) cytosolic fraction. $n = 6$; $^{***}P < 0.001$, Student's *t* test. Values are expressed as mean ± SEM.

to 76.0% ± 6.6% as compared with control ($P < 0.05$) (Figure 2, A and B), whereas knockdown of GSK3α did not affect *BACE1* mRNA expression ($P > 0.05$) (Figure 2, A and B). Additional exogenous expression of GSK3β rescued the reduction of *BACE1* expression resulting from knockdown of GSK3β by siRNA (Supplemental Figure 2). To examine whether specific knockdown of GSK3β expression also affected β-secretase processing of APP, we transfected siRNA specific to GSK3α or GSK3β into 20E2 cells while inhibiting γ-secretase activity with L658,458. Western blotting showed that GSK3α or GSK3β siRNA specifically reduced GSK3α or GSK3β expression, respectively (Figure 2C). Knockdown of GSK3α expression did not significantly affect BACE1-mediated APP processing, whereas GSK3β knockdown reduced the production of the BACE1 cleavage product C99 to 51.9% ± 6.4% ($P < 0.05$) (Figure 2, C and D).

To further confirm that GSK3β regulates *BACE1* gene expression at the transcription level, we assayed *BACE1* mRNA in the S9A-GSK3β inducible SHSY5Y stable cell line. This stable cell line carries the constitutively active mutant GSK3β, and expression of the mutant gene is under control of a tetracycline-inducible promoter (60). Addition of tetracycline induced the expression of active GSK3β (Figure 2E) and resulted in significantly increased expression of *BACE1* to 251.1% ± 70.0% relative to the control ($P < 0.05$) (Figure 2F). These data demonstrated that GSK3β, but not GSK3α, specifically regulates *BACE1* gene expression and contribute to APP processing.

GSK3β regulates BACE1 gene promoter activity. To investigate the molecular mechanism underlying the effect of GSK3β on *BACE1* gene expression at the transcription level, we performed a *BACE1* gene promoter assay. Two human *BACE1* gene promoter deletion plasmids were constructed. Regions of the *BACE1* promoter from –2890 to +292 bp (pB1-A) and from –9 to +292 bp (pB1-B) were inserted into promoterless vector pGL3-basic upstream of the firefly luciferase reporter gene (Figure 3A). To examine the effect of GSK3 on *BACE1* gene promoter activity, we transfected N2a cells with pB1-A and then treated them with ARA. Inhibition of GSK3 signaling by ARA significantly decreased the promoter activity of pB1-A in N2a cells to 54.9% ± 6.2% ($P < 0.005$) (Figure 3B). To further investigate the underlying mechanism and determine the *BACE1* promoter region that mediates the transcriptional activation by GSK3 signaling, we co-transfected N2a cells with either pB1-A or pB1-B plasmid together with the S9A-GSK3β plasmid, which carries a constitutively active form of GSK3β. Expression of active GSK3β markedly increased the luciferase activity of pB1-A in the S9A-GSK3β transfected cells to 144.0% ± 2.0% as compared with the control ($P < 0.05$), but had no significant effect on the luciferase activity of pB1-B ($P > 0.05$) (Figure 3C). This result showed that enhancing GSK3β signaling upregulated *BACE1* gene promoter activity and the 2.8-kb promoter region is responsible for GSK3β-mediated upregulation of *BACE1* transcription. To further confirm this finding, we transfected these two deletion promoter plasmids into *Gsk3b*-KO or wild-type cells. Ablation of *Gsk3b* expression in the *Gsk3b*-KO cells resulted in significant reduction in luciferase activity of pB1-A to 47.0% ± 7.5% as compared with the wild-type control cells ($P < 0.01$) (Figure 3D). However, knockout of the *Gsk3b* gene had no significant effect on the luciferase activity of pB1-B (Figure 3D). Taken together, these results demonstrated that GSK3β regulates *BACE1* gene expression via its effect on the *BACE1* promoter.

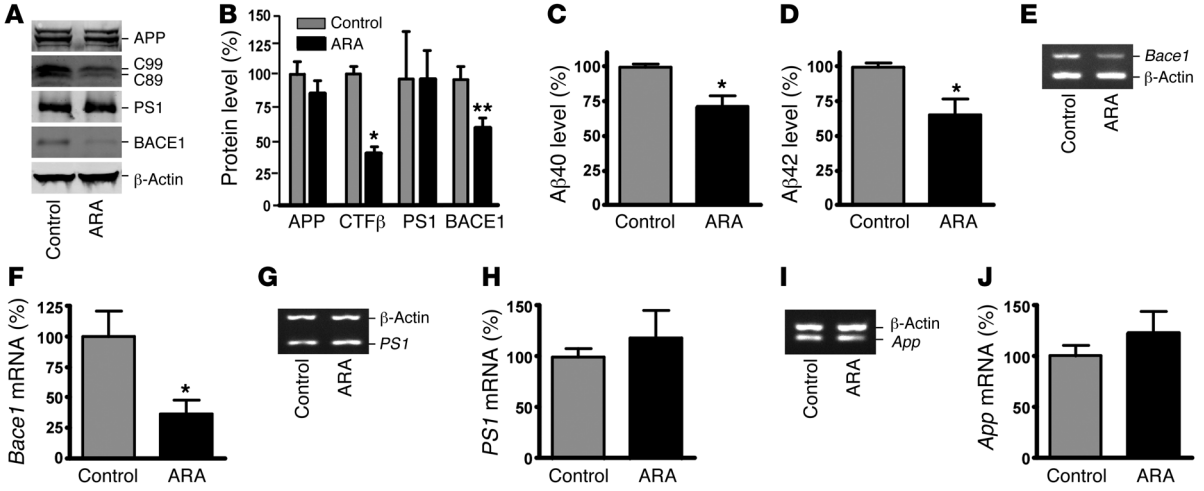

Figure 5

ARA inhibits BACE1 cleavage of APP and Aβ production in vivo. (**A**) Hemi-brains from ARA-treated and control APP23/PS45 mice of the 6 weeks age group were homogenized in RIPA-Doc lysis buffer and separated with 12% Tris-glycine or 16% Tris-tricine SDS-PAGE. Full-length APP and APP CTFs (C99 and C89) were detected by C20 polyclonal antibody. PS1 was detected by anti-PS1 N-terminal antibody 231. BACE1 was detected by anti-BACE1 antibody. β-Actin was detected by anti–β-actin antibody AC-15 as the internal control. (**B**) Quantification showed that CTFβ was significantly decreased in ARA-treated mice. $n = 25$ mice total. $^*P < 0.05$, $^{**}P < 0.01$, Student's t test. ELISA was performed to measure Aβ40 (**C**) and Aβ42 (**D**) levels from the brain tissues of APP23/PS45 mice injected with or without ARA. $n = 8$ for each group; $^*P < 0.005$, Student's t test. (**E**) Total RNA was isolated from APP23/PS45 mouse cortices by TRI Reagent. Sets of gene-specific primers were used to amplify *Bace1* (**E**), *PS1* (**G**), and *App* (**I**) genes. β-Actin was used as an internal control. *Bace1* mRNA levels were significantly reduced (**F**), while there were no difference in endogenous *PS1* (**H**) or *App* (**J**) mRNA levels between ARA-treated mice and controls. Values are expressed as mean ± SEM. $n = 12$ total; $^*P < 0.01$, Student's t test.

NF-κB mediates the transcriptional regulation of BACE1 gene expression by GSK3β. Recently we reported that levels of both BACE1 and NF-κB are increased in AD brains, and NF-κB signaling upregulates human *BACE1* gene expression by acting on the *cis*-acting p65-binding element in its promoter (27). Previous studies in *Gsk3b*-KO mice demonstrated that GSK3β is required for proper activation of NF-κB (61). As our data indicate that GSK3β regulates *BACE1* gene transcription, we next examined whether regulation of *BACE1* transcription by GSK3β signaling is dependent on NF-κB. TNF-α is a strong activator of NF-κB p65 expression. In order to examine the specific role of NF-κB in GSK3β-regulated *BACE1* transcription, we transfected N2a cells with a pBACE1-4κB promoter plasmid that contained only the NF-κB–binding elements in the human *BACE1* promoter (27). After transfection, the cells were cotreated with TNF-α and the GSK3 inhibitor ARA. ARA treatment alone consistently reduced *BACE1* promoter activity (Figure 4A). TNF-α stimulation increased pB1A promoter activity to 132.6% ± 7.5% of the control ($P < 0.01$). However, ARA treatment reduced the TNF-α–induced *BACE1* promoter activation to 115.6 ± 6.9% as compared with TNF-α treatment alone ($P < 0.05$) (Figure 4A). Overexpression of p65 NF-κB significantly increased the *BACE1* promoter activity to 487.1% ± 102.2% as compared with the control ($P < 0.001$) (Figure 3D). However, ARA did not affect NF-κB p65's upregulating effect on *BACE1* promoter activity ($P > 0.05$), indicating that GSK3 signaling may have its effect upstream of NF-κB in the modulation of *BACE1* transcription (Figure 4B). To further confirm ARA's effect on NF-κB activity, we co-transfected N2a cells with pNF-κB–Luc and NF-κB p65 or an empty vector, followed by treatment with ARA to inhibit GSK3 signaling. ARA reduced pNF-κB-Luc promoter activity to 51.9% ± 9.1% as compared with control ($P < 0.05$) (Figure 4C). Overexpression of NF-κB p65 significantly increased pNF-κB–Luc promoter activity to 203.36 ± 87.38–fold ($P < 0.001$) (Figure 4C). Additional ARA treatment did not have any significant effect on the transcriptional activation of pNF-κB–Luc by NF-κB p65 overexpression ($P > 0.05$) (Figure 4C). These data indicate that the p65-binding elements in the *BACE1* promoter mediated the effect of GSK3β on *BACE1* transcription.

To confirm the role of the NF-κB signaling pathway in GSK3β-mediated *BACE1* transcription, we transfected NF-κB p65 knockout RelA-KO cells and wild-type control cells with the *BACE1* promoter pB1-A and the constitutively active GSK3β expression plasmid S9A-GSK3β. In wild-type cells, activation of GSK3β signaling by expression of S9A-GSK3β markedly increased *BACE1* promoter activity to 189.6% ± 20.9% as compared with the vector control ($P < 0.05$), whereas activation of GSK3β signaling by expression of S9A-GSK3β had no effect on *BACE1* promoter activity in RelA-KO cells ($P > 0.05$) (Figure 4D), indicating that disruption of NF-κB p65 expression in RelA-KO cells abolished GSK3β's effect on the transcriptional activation of the human *BACE1* gene promoter. To further examine the effect of GSK3 inhibition on NF-κB p65 expression, we treated N2a cells with ARA and subjected them to subcellular fractionation (Figure 4E). ARA treatment significantly reduced nuclear NF-κB p65 levels to 46.9% ± 9.1% as compared with control ($P < 0.01$) (Figure 4F). Moreover, ARA treatment also reduced cytosolic NF-κB p65 levels to 56.1% ± 7.1% as compared with control ($P < 0.001$) (Figure 4G). These data show that GSK3 inhibition with ARA reduced NF-κB activity by decreasing NF-κB p65 levels. Taken together, our results demonstrate that NF-κB signaling mediates the regulatory effect of GSK3β on *BACE1* gene expression.

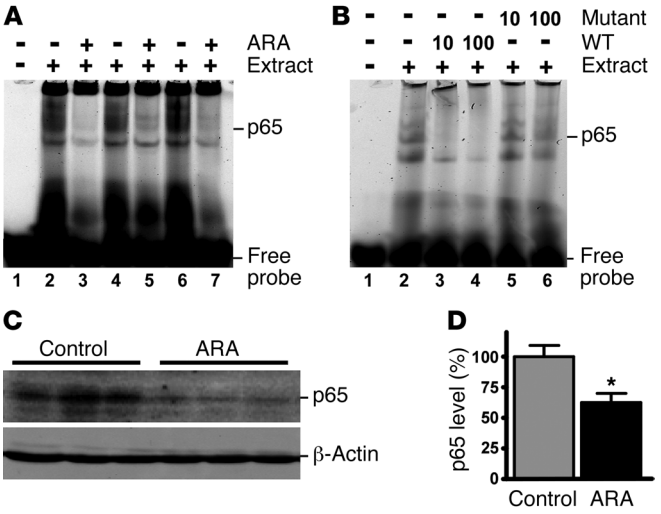

Figure 6
ARA reduced NF-κB binding in APP23/PS45 mouse brains. APP23/PS45 mice were injected daily with ARA for 4 weeks, and whole brain lysates were subjected to EMSA. (**A**) Mice that received ARA had reduced intensity of NF-κB shifted band. $n = 3$. (**B**) Whole brain lysates subjected to EMSA was competed with 10- and 100-fold excess of the wild-type and mutant NF-κB oligos to demonstrate the specificity of binding. (**C**) Daily injections of ARA to APP23/PS45 mice for 6 weeks reduced NF-κB p65 levels in the whole brain lysates. (**D**) Quantification of the band intensity of NF-κB p65 levels. Values are expressed as mean ± SEM. $n = 25$ total; $^*P < 0.005$.

GSK3 regulates BACE1 gene expression, APP processing, and Aβ production in vivo. Our data provide strong evidence that GSK3β activates *BACE1* gene expression, resulting in enhanced β-secretase processing of APP and Aβ production in vitro. To examine the effect of GSK3 signaling on *BACE1* gene expression and APP processing in vivo, we first assayed APP CTFs and Aβ production in the brain of APP23/PS45 mice by Western blot analysis (Figure 5, A and B). APP23/PS45 double transgenic mice, an AD mouse model, were generated by crossing APP23 mice, carrying the human Swedish mutant APP751 transgene driven by the neuron-specific Thy1.2 promoter, and PS45 mice, carrying the human familial AD–associated G384A mutant presenilin-1 (PS1) (54). The mice were treated with 5 mg/kg of the GSK3 inhibitor ARA at 6 weeks of age daily for 4 weeks, while age-matched control mice received vehicle solution. ARA treatment significantly decreased the brain levels of the β-secretase–generated CTFβ fragments C99 and C89, to 38.4% ± 4.8% relative to controls ($P < 0.05$) (Figure 5B). The levels of Aβ40 and Aβ42 were

Figure 7
AR-A014418 treatment significantly reduces neuritic plaque formation in AD transgenic mice. (**A** and **B**) APP23/PS45 double transgenic mice at the age of 6 weeks were treated with ARA (5 mg/kg) for 4 weeks, while age-matched control APP23/PS45 mice received vehicle solution. The mice were sacrificed after behavioral tests, and the brains were dissected, fixed, and sectioned. Neuritic plaques were detected using Aβ specific monoclonal antibody 4G8 (Signet). The plaques were visualized by microscopy with ×40 magnification. (**A**) A representative brain section of the control and (**B**) AR-A014418 injected APP23/PS45 mice sacrificed immediately after behavioral analysis. Black arrows point to plaques. Bars: 500 μm. The number of neuritic plaques was significantly reduced in AR-A014418 treated mice compared to controls. (**C**) Quantification of neuritic plaques in APP23/PS45 mice with treatment starting at the age of 6 weeks and sacrificed immediately after behavioral analysis, the number represents mean ± SEM, $n = 22$ mice total, $^*P < 0.01$ by Student's *t*-test. (**D** and **E**) Neuritic plaques were further confirmed using thioflavin S fluorescent staining and visualized by microscopy with a ×40 objective. There were less neuritic plaques in AR-A014418 treated mice (**E**) as compared to age matched control mice (**D**) sacrificed immediately after AR-A014418 injection. White arrows point to green fluorescent neuritic plaques. Bar: 500 μm. (**F** and **G**) Plaque formation in APP23/PS45 mice was further examined using 4G8 antibody staining 3 months after the last injection. (**F**) A representative brain section of control or (**G**) AR-A014418 injected APP23/PS45 mice sacrificed 3 months after the last injection. (**H**) Quantification of neuritic plaques in APP23/PS45 mice 3 months after the last injection. The number represents mean ± SEM, $n = 12$ mice total, $P > 0.05$ by Student's *t*-test.

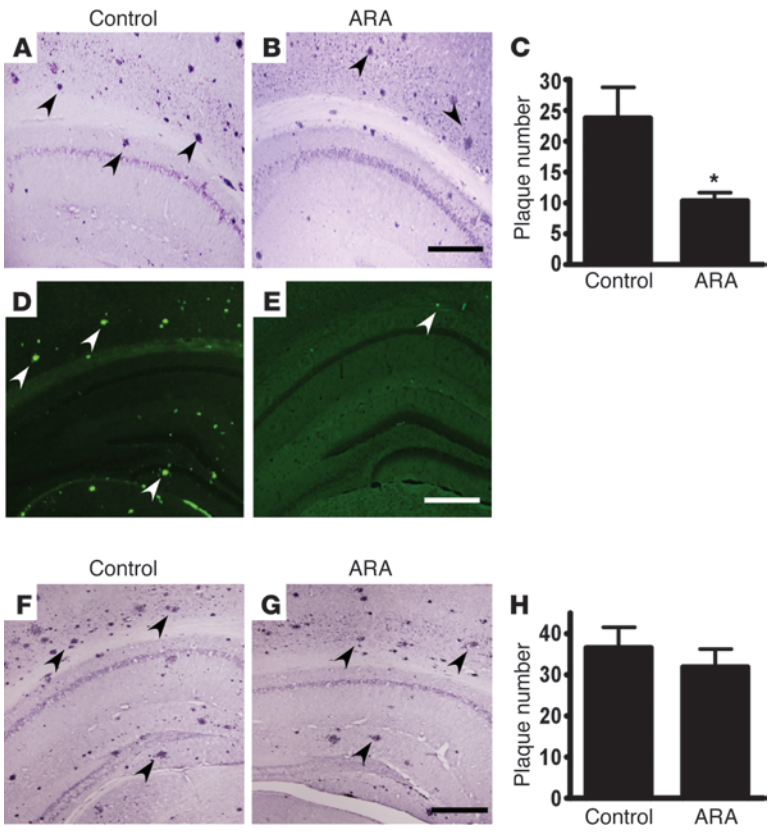

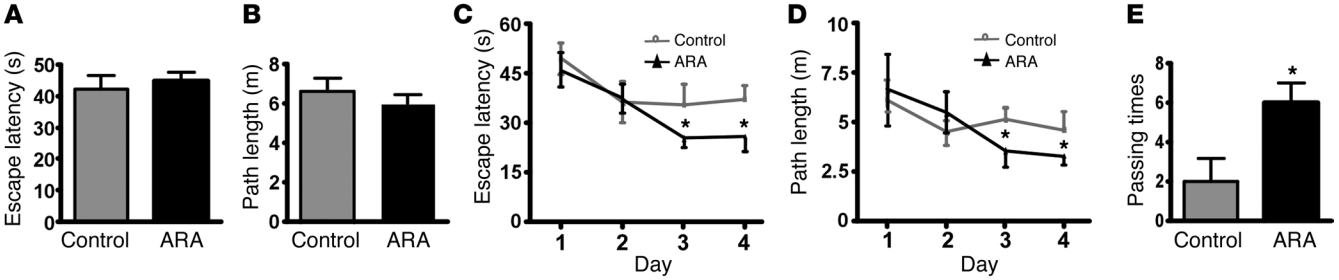

Figure 8

ARA improves memory deficits in AD transgenic mice. A Morris water maze test consists of 1 day of visible platform trials and 4 days of hidden platform trials, plus a probe trial 24 hours after the last hidden platform trial. Animal movement was tracked and recorded by ANY-maze tracking software. APP23/PS45 mice at 6 weeks were injected daily for 1 month with ARA or a vehicle solution and subjected to the Morris water maze test (n = 26 mice total, 14 ARA-treated and 12 sham-treated). (**A**) During the first day of visible platform tests, the ARA treated and control APP23/PS45 mice exhibited a similar latency to escape onto the visible platform. $P > 0.05$, Student's t test. (**B**) The ARA-treated and control APP23/PS45 mice had similar swimming distances before escaping onto the visible platform in the visible platform test. $P > 0.05$, Student's t test. (**C**) In hidden platform tests, mice were trained with 5 trials per day for 4 days. ARA-treated APP23/PS45 mice showed a shorter latency to escape onto the hidden platform on the third and fourth days. *$P < 0.05$, Tukey's post hoc analysis. (**D**) The ARA-treated APP23/PS45 mice had a shorter swimming length before escaping onto the hidden platform on the third and fourth days. *$P < 0.05$, Tukey's post hoc analysis. (**E**) In the probe trial on the sixth day, the ARA-treated APP23/PS45 mice traveled into the third quadrant, where the hidden platform was previously placed, significantly more times than controls. Values are expressed as mean ± SEM.*$P < 0.05$, Student's t test.

reduced to 71.2% ± 8.3% and 65.6% ± 11.0% in ARA-treated mice relative to controls, ($P < 0.05$) (Figure 5, C and D). These data demonstrate that inhibition of GSK3 activity by ARA treatment reduces β-secretase cleavage of APP and Aβ production in vivo.

We then examined whether the level of BACE1 was altered by GSK3 signaling in vivo. Western blot analysis showed that inhibition of GSK3 signaling significantly reduced the protein level of BACE1 to 64.7% ± 7.3% in ARA-treated mice, as compared with the control mice ($P < 0.01$), and the treatment had no significant effect on APP and PS1 protein levels ($P > 0.05$) (Figure 5, A and B). We further showed that GSK3 inhibition with ARA reduced tau phosphorylation, which is consistent with previous findings (ref. 62 and Supplemental Figure 1A). Our in vitro study has shown that GSK3β regulates the transcription of the *BACE1* gene. To confirm that the decrease in BACE1 protein level seen in the brains of the ARA-treated mice was due to reduced *BACE1* gene transcription, the endogenous *Bace1* mRNA levels were measured (Figure 5, E, G, and I). ARA treatment markedly reduced *Bace1* mRNA level to 36.7% ± 11.8% ($P < 0.01$) (Figure 5F), but did not significantly change the mRNA levels of *App* and *PS1* genes ($P > 0.05$) (Figure 5, H and J). These data demonstrate that, consistent with the in vitro results, inhibition of GSK3 specifically inhibited *Bace1* gene expression and its β-secretase activity in vivo.

Our study has demonstrated that NF-κB signaling is required for GSK3β's regulatory effect on *BACE1* gene expression in vitro. To confirm this effect in vivo, we examined whether NF-κB activity was affected in APP23/PS45 double transgenic mice administered ARA. EMSA was used to assess NF-κB consensus DNA binding in whole brain lysates. ARA treatment inhibited the binding of NF-κB p65 protein to the *cis*-acting consensus oligonucleotide probe, resulting in a reduction in the intensity of the p65 NF-κB shifted bands (Figure 6A). The specificity of the bands was confirmed by competition assay with addition of ×10 and ×100 unlabeled wild-type NF-κB oligonucleotides (oligos), while the mutant NF-κB oligos did not have any significant effect on the shifted bands (Figure 6B). Consistent with the in vitro experiment, APP23/PS45 mice receiving ARA treatment showed a significant reduction in NF-κB levels to 62.9% ± 6.9% of those in the sham-injected controls ($P < 0.005$) (Figure 6, C and D). Thus, inhibition of GSK3 signaling attenuates NF-κB binding to *cis*-acting p65 binding elements by reducing NF-κB levels in the AD transgenic model mice in vivo.

GSK3 inhibition reduces neuritic plaque formation in the AD model mice. To examine the specific effect of GSK3 signaling on AD pathogenesis, we treated APP23/PS45 double transgenic mice with ARA. The double transgenic mice develop detectable neuritic plaques in the neocortex and hippocampus as early as 1 month of age. The mice were treated with 5 mg/kg ARA at 6 weeks of age daily for 4 weeks, while age-matched control mice received vehicle solution. 4G8 immunostaining and thioflavin-S staining were used to detect Aβ-containing neuritic plaques in the brains (ref. 63 and Figure 7). ARA treatment significantly decreased the number of neuritic plaques in the transgenic mice relative to the vehicle-injected group (Figure 7, A and B). Quantification showed that overall ARA treatment reduced plaque number by approximately 50% (23.8 ± 4.7 vs. 10.4 ± 1.3 per slice, $P < 0.01$) (Figure 7C). Thioflavin-S staining also confirmed that ARA treatment dramatically reduced the number of Aβ-containing neuritic plaques in the brains of APP23/PS45 double transgenic mice (Figure 7, D and E). The inhibitory effect of ARA was reversible, and the treated mice (Figure 7G) had plaque numbers similar to those in the control mice (Figure 7F) when examined 3 months after the end of the drug treatment (36.5 ± 5.1 vs. 32.1 ± 4.2, $P > 0.05$) (Figure 7H). During the 4-week injection period, ARA treatment of the mice did not affect food consumption, and no significant weight changes were observed between the treatment and control groups (data not shown).

Inhibition of GSK3 significantly improves memory deficits in the AD model mice. To investigate whether GSK3 inhibition by ARA treatment affects the memory deficit in AD pathogenesis, we used the Morris water maze to test spatial memory after APP23/PS45 mice received 1 month of ARA treatment (64). In the visible platform tests, ARA-treated and control APP23/PS45 mice had similar escape latency (42.4 ± 4.3 and 44.8 ± 2.7 seconds, $P > 0.05$) (Figure 8A) and path length (6.6 ± 0.7 m and 6.1 ± 0.5 m, $P > 0.05$) (Figure

8B), indicating that ARA treatment did not affect mouse mobility or vision. In the hidden platform test, ARA-treated mice showed significant improvements as compared with the vehicle-treated controls. The escape latency on the third and fourth days of the hidden platform test was shorter (12.0 ± 1.6 and 17.4 ± 3.1 seconds) than that of sham-treated mice (23.8 ± 4.0 s and 24.9 ± 2.7 s) ($P < 0.05$, Figure 8C). The ARA-treated mice swam significantly shorter distances to reach the platform (2.9 ± 0.7 m and 3.2 ± 0.3 m) as compared with control mice (3.7 ± 0.6 and 4.2 ± 0.5 m) on the third and fourth days ($P < 0.05$, Figure 8D). In the probe trial on the last day of testing, the platform was removed. ARA treatment significantly improved the spatial memory in the APP23/PS45 mice, as these mice spent more time searching for the platform in the appropriate quadrant (Supplemental Figure 3A). The number of times the mice traveled into the third quadrant, where the hidden platform was previously placed, was significantly greater with ARA treatment as compared with control (6.0 ± 1.0 and 2.0 ± 1.2 times, $P < 0.05$) (Figure 8E). Moreover, ARA-treated mice spent nearly twice as long in the southwest (SW) quadrant, where the platform was originally placed during the hidden platform test (NE 16.3.9% ± 1.3%, SE 19.2% ± 1.6%, SW 44.0% ± 3.1%, NW 20.4% ± 2.0%). The sham-treated mice, however, spent approximately equal amounts of time in each quadrant (NE 24.9% ± 1.9%, SE 20.4% ± 2.0%, SW 28.2% ± 1.7%, NW 26.6% ± 2.1%) (Supplemental Figure 3B). These data demonstrate that inhibition of GSK3 signaling significantly improved the memory deficits seen in the AD model mice.

Discussion

GSK3 signaling has been previously shown to be strongly associated with several neuropathological changes of AD. GSK3 is involved in tau hyperphosphorylation (65), neuronal apoptosis (66), and synaptic dysfunction (67). Moreover, GSK3 signaling has also been implicated in Aβ production and neuritic plaque formation (51, 54, 68). However, the mechanism by which GSK3 affects APP processing and Aβ production has not been clearly elucidated, and its pharmaceutical potential as an effective drug target remains to be validated. The current study clearly indicates that GSK3β, but not the related GSK3α isoform, facilitates Aβ production by upregulating *BACE1* gene expression via NF-κB p65 *cis*-acting elements on the *BACE1* gene promoter. The C-terminal end of BACE1 undergoes phosphorylation, which regulates BACE1 trafficking and cellular levels (69, 70). In our study, inhibition of GSK3 signaling did not affect the phosphorylation status of BACE1 (data not shown). Thus, specifically inhibiting GSK3 decreases BACE1 expression and markedly reduces β-secretase processing of APP and Aβ production, resulting in inhibition of neuritic plaque formation and amelioration of memory deficits in AD model mice.

GSK3 appears to be a common molecular link between amyloidogenesis and tau abnormalities in AD pathology. Therefore, GSK3 inhibition has been proposed to be a valid therapeutic target for treating AD. Lithium chloride and valproic acid are known to have some inhibitory effects on GSK3 (71, 72) and have been used in the clinic for many decades for the treatment of bipolar disorders and epilepsy. Recent work has demonstrated that lithium and valproic acid could reduce Aβ levels and improve cognitive performance in mouse models of AD (54, 68). While the inhibitory effects of lithium and valproic acid on GSK3 are known, both compounds have also been found to affect signaling cascades independent of GSK3. To further investigate the role of GSK3 on APP processing, we administered ARA, a highly selective and potent inhibitor of GSK3 (IC_{50} = 104 ± 27 nM) (73) to APP Swedish stable cell lines and APP23/PS45 mice. We found that with specific GSK3 inhibition, the BACE1 major product C99 is reduced, accompanied by a significant reduction in Aβ levels. Previous reports indicated that ARA treatment reduced tau hyperphosphorylation and tangle formation in transgenic mice overexpressing human tau, a model of AD (62). Our study shows that ARA also reduces plaque pathology and rescues cognitive deficits in an AD mouse model. However, continuous ARA treatment is required in order to reduce plaque pathology, as APP23/PS45 mice sacrificed 3 months after the last injection had plaque levels similar to those in the control group.

Previous work by Phiel et al. (51) demonstrated that inhibition of GSK3α with isoform-specific siRNA decreases γ-secretase activity but found no effect of GSK3β. In our study, we found that in a system in which γ-secretase activity is pharmacologically inhibited, GSK3α knockdown did not have any significant effect on APP processing. On the other hand, GSK3β knockdown with inhibition of γ-secretase activity reduced the level of C99 fragment, indicating that BACE1 activity is affected. We further provided evidence that knocking down GSK3β reduced *BACE1* mRNA levels, but knocking down GSK3α did not affect *BACE1* expression. Previous genetic studies have found that during development GSK3α could not compensate for the loss of GSK3β, as *Gsk3b*-KO mice are embryonic lethal while *Gsk3a*-KO mice are viable (61). This argues that GSK3α and GSK3β isoforms may have distinct cellular functions with respect to BACE1 expression. Moreover, GSK3β is the predominant isoform in the brain and therefore has been implicated in many CNS disorders (74). However, Jaworski et al. recently showed the GSK3α/β knockout mice did not show any changes to APP processing and Aβ production (52). This could be due to a physiological compensation of BACE1 expression in the KO mice compared with the acute effect of the GSK3 inhibitor. Additionally, our data showed that GSK3β regulated NF-κB–mediated BACE1 expression. *Gsk3a* knockout had no effect on NF-κB signaling. Taken together, these studies suggest that GSK3 isoforms have distinct roles in regulating APP processing. We do not believe that gene silencing of GSK3 isoforms would be a valid approach for treating AD. Complete ablation of each isoform may lead to compensatory elevated activity of the other isoform or even other functionally protein kinases. Moreover, it has been reported that complete ablation of GSK3α/β expression in mice results in various abnormalities (75), which may interfere with any therapeutic values.

Epidemiological and experimental studies have suggested a significant inflammatory component in AD (76–79). However, it remains controversial whether neuroinflammation is a driving force for AD or simply a byproduct of the disease (80). Moreover, the detrimental role of astrocyte and microglia during neuroinflammation remains elusive. The release of various proinflammatory and anti-inflammatory cytokines has been shown to affect APP processing, Aβ production, and neurodegenerative changes in AD brains. There have been preclinical studies to show that nonsteroidal anti-inflammatory drugs (NSAIDs) or anti-inflammatory cytokines have beneficial effects in treating AD (80, 81). However, there are reports demonstrating that anti-inflammatory stimuli could potentiate Aβ production, possibly through suppression of glia-mediated Aβ clearance. On the other hand, proinflammatory stimuli could also have extreme effects on AD pathogenesis. There

is a large amount of evidence to show that increased proinflammatory cytokines correlates with Aβ production and neurodegeneration. In contrast, there are also a number of studies indicating that proinflammatory cytokines precondition the system for Aβ challenge and protect against neurodegeneration (82–85). Clearly, inflammation is a major component of the AD brain, and more work will be required in order to elucidate its role in AD pathogenesis. Since several proinflammatory cytokines including the interleukins and TNF have been found to activate GSK3β, and GSK3 inhibitors showed anti-inflammatory effects (86–88), we speculate that GSK3 plays an important role in the inflammatory response driving Aβ production.

The chronic inflammatory response induced by Aβ may depend on transcription factors to exert neurodegenerative effects. Regulation of the transcription factor NF-κB and its transcriptional activity may in part play a role in Aβ-mediated neurodegeneration (27, 89). It has been previously reported that the *BACE1* promoter contains NF-κB–binding elements (27, 90) and exacerbated Aβ levels modulate the *BACE1* promoter activity via NF-κB–dependent pathways (91). More recently, Chen et al. (27) found increased NF-κB p65 and BACE1 expression in postmortem AD brains. Furthermore, overexpression of NF-κB p65 was found to increase human *BACE1* promoter activity, whereas inhibiting NF-κB signaling reduced *BACE1* expression (27).

Exogenous application of Aβ has been found to increase GSK3β activity and NF-κB levels. There are many reports suggesting that GSK3β regulates gene transcription in an NF-κB–dependent manner (61, 92, 93). Therefore, we argue that the GSK3β/NF-κB signaling pathway is involved in regulating *BACE1* gene transcription. In this study, we found that interfering with GSK3β activity using *Gsk3b*-KO cells or ARA treatment reduced *BACE1* promoter activity and gene expression. Moreover, disrupting NF-κB expression also blocked GSK3β-induced *BACE1* transcription.

Long-term treatment with GSK3 inhibitors always raises the concern about unwanted side effects. Many of the Wnt signal transduction components such as the *APC* gene or β-catenin gene carry mutations that render the protein nondegradable (94). Prolonged activation of the Wnt pathway has been linked to development of various cancers (95). GSK3 inhibitors including SB216763, SB415286, Kenpaullone, and lithium chloride have all been shown to elevate the level of β-catenin (51, 96, 97). Consequently, it may be possible that GSK3 inhibitors may mimic Wnt signaling and could potentially be oncogenic. However, long-term use of lithium chloride to treat bipolar disorder has not been linked to increased risk of cancer. Interestingly, administration of the GSK3 inhibitors CHIR99021 and ARA did not change β-catenin levels (65). Moreover, β-catenin levels are largely unaffected in *Gsk3b*-KO embryos (61). These findings indicate that the inhibition of GSK3 by itself might not be sufficient to elevate the level of β-catenin. It is possible that there are specific pools of GSK3 that are insensitive to certain GSK3 inhibitors, thereby sparing the effect of increasing β-catenin levels. In order to validate the therapeutic efficacy of GSK3 inhibition, while minimizing oncogenic side effects, long-term treatment studies in cells and animals will be required.

In conclusion, we have found that the GSK3β/NF-κB signaling pathway regulates *BACE1* transcription and thereby facilitates Aβ production in AD. Since GSK3β and NF-κB are involved in AD pathogenesis, our results suggest that direct interference of this pathway may be a promising drug target for AD therapy.

Methods

Cell culture, transfection, and ARA treatment. All cells were maintained at 37°C in an incubator containing 5% CO_2. HEK293 (human embryonic kidney), N2a (mouse neuroblastoma), SHSY5Y (human neuroblastoma), and wild-type MEFs (mouse embryonic fibroblasts) were maintained in complete DMEM supplemented with 10% fetal bovine serum, 1% L-glutamine, 1% penicillin/streptomycin, and 1% sodium pyruvate (Invitrogen). G*sk3b*-KO fibroblast cells were derived from E12.5 G*sk3b*-KO mouse embryos and were maintained in complete DMEM (61). The 20E2 cell line is a Swedish mutant APP695 stable HEK293 cell line cultured in complete DMEM with 50 μg/ml geneticin (98). 293B2 cells stably expressing human *BACE1* in HEK293 cell line were cultured in complete DMEM with 100 μg/ml Zeocin (99). The RelA-KO fibroblast cell line, derived from E12.5–E14.5 mouse embryo fibroblasts, was maintained in DMEM supplemented with 15% FBS, β-mercaptoethanol, and ESGRO (LIF) (100). S9A-GSK3β stably transfected SHSY5Y cells, under the control of the tetracycline-regulated mammalian expression T-Rex system (Invitrogen), were maintained in complete DMEM (60). S9A-GSK3β gene induction was achieved by stimulation with 1 μg/ml tetracycline (60). Cells were transfected with plasmid DNA using either calcium phosphate or Lipofectamine 2000 (Invitrogen). L685,458, G2, and ARA (EMD Biosciences) were dissolved in DMSO and diluted with complete cell culture medium. The final DMSO concentrations in each experiment were less than 0.5%.

Luciferase assay. *BACE1* promoter constructs were transfected into N2a cells and wild-type and *Gsk3b*-KO MEFs. The *Renilla* (sea pansy) luciferase vector pCMV-Rluc was co-transfected to normalize transfection efficiency. A luciferase assay was performed 48 hours after transfection with the Dual-Luciferase Reporter Assay system (Promega) as previously described (27).

Semiquantitative RT-PCR. RNA was isolated from cells using TRI Reagent (Sigma-Aldrich). A Thermoscript Reverse Transcription kit (Invitrogen) was used to synthesize the first-strand cDNA from an equal amount of RNA following the manufacturer's instructions. The newly synthesized cDNA templates were further amplified via Platinum *Taq* DNA polymerase in a 20-μl reaction. The following primers were used to specifically amplify *BACE1*, *GSK3A*, *GSK3B*, *APP*, and *PS1* genes: *BACE1* forward 5′-cccgcagacgctcaacatcc and reverse 5′-GCCACTGTCCACAATGCTCTT; *GSK3A* forward 5′-TGAAGCTGGGCCGTGACAGCGG and reverse 5′-ACATGTACACCTTGACATAG; *GSK3B* forward 5′-TCAGGAGTGCGGGTCTTCCGAC and reverse 5′-CTCCAGTATTAGCATCTGACGCT; *APP* forward 5′-GCTGGCCTGCTGGCTGAACC and reverse 5′-GGCGACGGTGTGCCAGTGAA; *PS1* forward 5′-GAGACACAGGACAGTGGTTCTGG and reverse 5′-GGCCGATCAGTATGGCTACAAA. β-Actin was used as an internal control. The samples were resolved and analyzed on a 1.2% agarose gel.

Immunoblot analysis. Brain tissues or cells were lysed in RIPA lysis buffer (1% Triton X-100, 1% sodium deoxycholate, 4% SDS, 0.15 M NaCl, 0.05 M Tris-HCl, pH 7.2) supplemented with 200 mM sodium orthovanadate, 25 mM β-glycerophosphate, 20 mM sodium pyrophosphate, 30 mM sodium fluoride, 1 mM PMSF, and a complete Mini Protease Inhibitor Cocktail Tablet (Roche Diagnostics). The samples were diluted in 4× SDS-sample buffer, boiled, and resolved on 12% Tris-glycine SDS-PAGE or 16% Tris-tricine SDS-PAGE, followed by transfer to polyvindylidine fluoride (PVDF-FL) membranes. For immunoblot analysis, membranes were blocked for 1 hour in PBS containing 5% nonfat dried milk, followed by overnight incubation at 4°C in primary antibodies diluted in the blocking medium. Rabbit anti-APP C-terminal polyclonal antibody C20 was used to detect APP and its CTF products. PS1 was detected by anti-PS1 N-terminal antibody 231. Total GSK3β was determined using a pan-specific mouse anti-GSK3α/β antibody (BioSource International Inc.). Total β-catenin was determined using a pan-specific rabbit anti–β-catenin antibody (Cell Signaling Technology). The NF-κB p65 subunit was determined using mouse

anti-p65 (Sigma-Aldrich). Internal control β-actin was analyzed using monoclonal antibody AC-15 (Sigma-Aldrich). BACE1 was detected with the anti-BACE1 antibody 208 recognizing the C-terminal end (101).

Aβ40/42 ELISA. HEK293 cells stably expressing the human *APP* gene containing the Swedish mutation were maintained in cell culture medium supplemented with 1% FBS. Following ARA treatment for 24 hours, conditioned medium was harvested, and protease inhibitors and AEBSF (Roche Diagnostics) were added to prevent degradation of Aβ peptides. APP23/PS45 double transgenic mouse cortical tissues were prepared according to the manufacturer's instructions prior to carrying out the ELISA protocol (Invitrogen). The concentration of Aβ40 and Aβ42 were detected using an Aβ1–40 or Aβ1–42 Colorimetric ELISA kit (Invitrogen) according to the manufacturer's instructions.

EMSA. Whole brain extracts were prepared by homogenizing the tissue in Buffer C (20 mM HEPES pH 7.5, 400 mM NaCl, 1 mM EDTA, 1 mM EGTA, 1 mM DTT, 1 mM PMSF, 10% glycerol) supplemented with protease inhibitor. EMSA was performed as previously described with a few changes (102). Briefly, 20–40 μg protein was incubated with an IRDye 700–labeled NF-κB oligo (5′-AGTTGAGGGGACTTTCCCAGGC), and the gels were scanned using the Odyssey system (LI-COR Biosciences). In the competition assay, unlabeled wild-type and mutant (5′-AGTTGAGGC-CACTTTCCCAGGC) NF-κB oligos at ×10 and ×100 molar excess were used to compete for binding.

Transgenic mice and drug treatment. APP23 mice overexpressing the Swedish APP_{751} (KM→NL) mutant transgene driven by the mouse Thy1.2 promoter were originally generated at Novartis Pharma as previously described (30, 103). APP23/PS45 double transgenic mice were generated by crossing APP23 mice with mice overexpressing the human G384A-mutated PS1 under the control of the murine Thy1 promoter (B6,D2-TgN(Thy1-$PS1_{G384A}$)45) (54, 103–105). APP23 and PS45 mice had been backcrossed to C57BL/6 mice for more than 7 generations prior to breeding for the double transgenic mice. The genotype of the mice was confirmed by PCR using DNA from tail tissues. The treatment group contained 14 animals (8 females, 6 males), and the sham-injected group contained 12 animals (7 females, 5 males). The treatment group received 5 mg/kg ARA diluted in 0.9% saline daily via intraperitoneal injection at the same time each day. Mice in the control group were injected with the vehicle solution containing DMSO diluted in 0.9% saline only. We tabulated the daily food consumption and weight for each mouse.

Immunohistochemical staining. Mice were sacrificed after behavioral testing, and half brains were immediately homogenized for protein, RNA, or DNA extraction. The other halves of the brains were fixed in 4% paraformaldehyde and sectioned with a Leica Cryostat to 30-μm thickness. Every twelfth slice with the same reference position was mounted onto slides for staining. Immunocytochemical staining was performed on floating sections. The plaques in the sections were detected with biotinylated monoclonal 4G8 antibody (Signetlabs) in 1:500 dilution, visualized by the ABC and DAB method, and counted under a ×40 objective as previously described (54, 63). Plaques were quantified, and the average plaque count per slice was recorded for each mouse. Thioflavin-S staining of plaques was performed with 1% thioflavin-S visualized using fluorescence microscopy (54).

Morris water maze test. The Morris water maze test was performed as previously described (30, 64). The APP23/PS45 mice treated with or without ARA were subjected to the Morris water maze test 1 day after the last injection regimen. The test was performed in a 1.5-meter-diameter pool with a 10-cm-diameter platform placed in the SE quadrant of the pool. The procedure consisted of 1 day of visible platform tests and 4 days of hidden platform tests, plus a probe trial 24 hours after the last hidden platform test. In the visible platform test performed on the first day, the mice were tested for 5 continuous trials, with an inter-trial interval of 60 minutes. In the hidden platform tests, mice were trained for 5 trials, with an inter-trial interval of 1 hour. Each mouse was allowed 60 seconds to search for the platform. In the scenario where the mouse could not locate the platform, the experiment guided it to the platform and allowed the mouse to rest there for 15 seconds. On the last day of the test, each mouse was subjected to the probe trial in which the platform was removed. Each mouse was given 60 seconds to locate where the platform was originally placed. Mouse behavior including distance traveled, escape latency and the number of passes through the platform was recorded by automated video tracking (ANY-maze, Stoelting). The data were analyzed by 2-way ANOVA, followed by Tukey's post hoc test.

Statistics. All results were presented as mean ± SEM and analyzed by ANOVA or 2-tailed Student's *t*-test. Statistical significance is accepted when $P < 0.05$.

Study approval. Animal experiments were conducted in accordance with the University of British Columbia Animal Care and Use Committee and Canadian Institutes of Health Research (CIHR) guidelines.

Acknowledgments

We thank Steven R. Vincent and Jing Zhang for helpful comments. This work is supported by the Canadian Institutes for Health Research (CIHR) (MOP-97825 and TAD-117948), the National Natural Science Foundation of China (NSFC) (NSFC81161120498), and the Jack Brown and Family Alzheimer's Research Foundation. W. Song is the holder of the Tier 1 Canada Research Chair in Alzheimer's Disease. P.T.T. Ly is supported by the Natural Sciences and Engineering Research Council (NSERC) Alexander Graham Bell Canada Graduate Scholarship and Michael Smith Foundation for Health Research (MSFHR) Senior Graduate Studentship. Y. Wu is the recipient of the Arthur and June Willms Fellowship. R. Wang and Y. Yang are supported by the Chinese Scholarship Council award.

Received for publication April 26, 2012, and accepted in revised form September 27, 2012.

Address correspondence to: Weihong Song, Department of Psychiatry, The University of British Columbia, 2255 Wesbrook Mall, Vancouver, British Columbia V6T 1Z3, Canada. Phone: 604.822.8019; Fax: 604.822.7756; E-mail: weihong@mail.ubc.ca.

1. Sinha S, et al. Purification and cloning of amyloid precursor protein beta-secretase from human brain. *Nature*. 1999;402(6761):537–540.
2. Hussain I, et al. ASP1 (BACE2) cleaves the amyloid precursor protein at the beta-secretase site. *Mol Cell Neurosci*. 2000;16(5):609–619.
3. Yan R, et al. Membrane-anchored aspartyl protease with Alzheimer's disease beta-secretase activity. *Nature*. 1999;402(6761):533–537.
4. Vassar R, et al. Beta-secretase cleavage of Alzheimer's amyloid precursor protein by the transmembrane aspartic protease BACE. *Science*. 1999; 286(5440):735–741.
5. Li Y, Zhou W, Tong Y, He G, Song W. Control of APP processing and Abeta generation level by BACE1 enzymatic activity and transcription. *FASEB J*. 2006;20(2):285–292.
6. von Arnim CAF, et al. The low density lipoprotein receptor-related protein (LRP) is a novel beta-secretase (BACE1) substrate. *J Biol Chem*. 2005; 280(18):17777–17785.
7. Li Q, Sudhof TC. Cleavage of amyloid-beta precursor protein and amyloid-beta precursor-like protein by BACE 1. *J Biol Chem*. 2004;279(11):10542–10550.
8. Pastorino L, et al. BACE (beta-secretase) modulates the processing of APLP2 in vivo. *Mol Cell Neurosci*. 2004;25(4):642–649.
9. Kitazume S, Tachida Y, Oka R, Shirotani K, Saido TC, Hashimoto Y. Alzheimer's beta-secretase, beta-site amyloid precursor protein-cleaving enzyme, is responsible for cleavage secretion of a Golgi-resident sialyltransferase. *Proc Natl Acad Sci U S A*. 2001;98(24):13554–13559.
10. Lichtenthaler SF, et al. The cell adhesion protein P-selectin glycoprotein ligand-1 is a substrate for the aspartyl protease BACE1. *J Biol Chem*. 2003;278(49):48713–48719.
11. Christensen MA, Zhou W, Qing H, Lehman A, Philipsen S, Song W. Transcriptional regulation of

BACE1, the beta-amyloid precursor protein beta-secretase, by Sp1. *Mol Cell Biol*. 2004;24(2):865–874.
12. Sun X, et al. Distinct transcriptional regulation and function of the human BACE2 and BACE1 genes. *FASEB J*. 2005;19(7):739–749.
13. Zhou W, Song W. Leaky scanning and reinitiation regulate BACE1 gene expression. *Mol Cell Biol*. 2006;26(9):3353–3364.
14. De Pietri Tonelli D, Mihailovich M, Di Cesare A, Codazzi F, Grohovaz F, Zacchetti D. Translational regulation of BACE-1 expression in neuronal and non-neuronal cells. *Nucleic Acids Res*. 2004; 32(5):1808–1817.
15. Lammich S, Schobel S, Zimmer AK, Lichtenthaler SF, Haass C. Expression of the Alzheimer protease BACE1 is suppressed via its 5′-untranslated region. *EMBO Rep*. 2004;5(6):620–625.
16. Rogers GW Jr, Edelman GM, Mauro VP. Differential utilization of upstream AUGs in the beta-secretase mRNA suggests that a shunting mechanism regulates translation. *Proc Natl Acad Sci U S A*. 2004;101(9):2794–2799.
17. Shi J, et al. The 1239G/C polymorphism in exon 5 of BACE1 gene may be associated with sporadic Alzheimer's disease in Chinese Hans. *Am J Med Genet*. 2004;124B(1):54–57.
18. Clarimon J, Bertranpetit J, Calafell F, Boada M, Tarraga L, Comas D. Association study between Alzheimer's disease and genes involved in Abeta biosynthesis, aggregation and degradation: suggestive results with BACE1. *J Neurol*. 2003;250(8):956–961.
19. Kirschling CM, Kolsch H, Frahnert C, Rao ML, Maier W, Heun R. Polymorphism in the BACE gene influences the risk for Alzheimer's disease. *Neuroreport*. 2003;14(9):1243–1246.
20. Cruts M, et al. Amyloid beta secretase gene (BACE) is neither mutated in nor associated with early-onset Alzheimer's disease. *Neurosci Lett*. 2001;313(1–2):105–107.
21. Nicolaou M, et al. Mutations in the open reading frame of the beta-site APP cleaving enzyme (BACE) locus are not a common cause of Alzheimer's disease. *Neurogenetics*. 2001;3(4):203–206.
22. Zhou W, et al. BACE1 gene promoter single-nucleotide polymorphisms in Alzheimer's disease. *J Mol Neurosci*. 2010;42(1):127–133.
23. Russo C, et al. Presenilin-1 mutations in Alzheimer's disease. *Nature*. 2000;405(6786):531–532.
24. Holsinger RM, McLean CA, Beyreuther K, Masters CL, Evin G. Increased expression of the amyloid precursor beta-secretase in Alzheimer's disease. *Ann Neurol*. 2002;51(6):783–786.
25. Yang LB, et al. Elevated beta-secretase expression and enzymatic activity detected in sporadic Alzheimer disease. *Nat Med*. 2003;9(1):3–4.
26. Fukumoto H, Rosene DL, Moss MB, Raju S, Hyman BT, Irizarry MC. Beta-secretase activity increases with aging in human, monkey, and mouse brain. *Am J Pathol*. 2004;164(2):719–725.
27. Chen CH, et al. Increased NF-kappaB signalling up-regulates BACE1 expression and its therapeutic potential in Alzheimer's disease. *Int J Neuropsychopharmacol*. 2012;15(1):77–90.
28. Zhao J, et al. Beta-site amyloid precursor protein cleaving enzyme 1 levels become elevated in neurons around amyloid plaques: implications for Alzheimer's disease pathogenesis. *J Neurosci*. 2007;27(14):3639–3649.
29. Wang W-X, et al. The expression of microRNA miR-107 decreases early in Alzheimer's disease and may accelerate disease progression through regulation of beta-site amyloid precursor protein-cleaving enzyme 1. *J Neurosci*. 2008;28(5):1213–1223.
30. Sun X, et al. Hypoxia facilitates Alzheimer's disease pathogenesis by up-regulating BACE1 gene expression. *Proc Natl Acad Sci U S A*. 2006; 103(49):18727–18732.
31. Luo Y, et al. Mice deficient in BACE1, the Alzheimer's beta-secretase, have normal phenotype and abolished beta-amyloid generation. *Nat Neurosci*. 2001;4(3):231–232.
32. Cai H, et al. BACE1 is the major beta-secretase for generation of Abeta peptides by neurons. *Nat Neurosci*. 2001;4(3):233–234.
33. Roberds SL, et al. BACE knockout mice are healthy despite lacking the primary beta-secretase activity in brain: implications for Alzheimer's disease therapeutics. *Hum Mol Genet*. 2001;10(12):1317–1324.
34. Kao S-C, Krichevsky AM, Kosik KS, Tsai L-H. BACE1 suppression by RNA interference in primary cortical neurons. *J Biol Chem*. 2004;279(3):1942–1949.
35. Ohno M, et al. BACE1 deficiency rescues memory deficits and cholinergic dysfunction in a mouse model of Alzheimer's disease. *Neuron*. 2004;41(1):27–33.
36. Hussain I, et al. Oral administration of a potent and selective non-peptidic BACE-1 inhibitor decreases beta-cleavage of amyloid precursor protein and amyloid-beta production in vivo. *J Neurochem*. 2007;100(3):802–809.
37. Hu X, et al. Bace1 modulates myelination in the central and peripheral nervous system. *Nat Neurosci*. 2006;9(12):1520–1525.
38. Willem M, et al. Control of Peripheral Nerve Myelination by the {beta}-Secretase BACE1. *Science*. 2006;314(5799):664–666.
39. McConlogue L, et al. Partial reduction of BACE1 has dramatic effects on Alzheimer plaque and synaptic pathology in APP Transgenic Mice. *J Biol Chem*. 2007;282(36):26326–26334.
40. Cohen P, Goedert M. GSK3 inhibitors: development and therapeutic potential. *Nat Rev Drug Discov*. 2004;3(6):479–487.
41. Doble BW, Woodgett JR. GSK-3: tricks of the trade for a multi-tasking kinase. *J Cell Sci*. 2003; 116(pt 7):1175–1186.
42. Leroy K, Boutajangout A, Authelet M, Woodgett JR, Anderton BH, Brion JP. The active form of glycogen synthase kinase-3beta is associated with granulovacuolar degeneration in neurons in Alzheimer's disease. *Acta Neuropathol*. 2002;103(2):91–99.
43. Hughes K, Nikolakaki E, Plyte SE, Totty NF, Woodgett JR. Modulation of the glycogen synthase kinase-3 family by tyrosine phosphorylation. *EMBO J*. 1993;12(2):803–808.
44. Cross DA, Alessi DR, Cohen P, Andjelkovich M, Hemmings BA. Inhibition of glycogen synthase kinase-3 by insulin mediated by protein kinase B. *Nature*. 1995;378(6559):785–789.
45. Cross DA, Alessi DR, Vandenheede JR, McDowell HE, Hundal HS, Cohen P. The inhibition of glycogen synthase kinase-3 by insulin or insulin-like growth factor 1 in the rat skeletal muscle cell line L6 is blocked by wortmannin, but not by rapamycin: evidence that wortmannin blocks activation of the mitogen-activated protein kinase pathway in L6 cells between Ras and Raf. *Biochem J*. 1994;1:21–26.
46. Rubinfeld B, Albert I, Porfiri E, Fiol C, Munemitsu S, Polakis P. Binding of GSK3beta to the APC-beta-catenin complex and regulation of complex assembly. *Science*. 1996;272(5264):1023–1026.
47. Chen RH, Ding WV, McCormick F. Wnt signaling to beta-catenin involves two interactive components. Glycogen synthase kinase-3beta inhibition and activation of protein kinase C. *J Biol Chem*. 2000;275(23):17894–17899.
48. Pei JJ, et al. Distribution of active glycogen synthase kinase 3beta (GSK-3beta) in brains staged for Alzheimer disease neurofibrillary changes. *J Neuropathol Exp Neurol*. 1999;58(9):1010–1019.
49. Ishiguro K, et al. Glycogen synthase kinase 3 beta is identical to tau protein kinase I generating several epitopes of paired helical filaments. *FEBS Lett*. 1993;325(3):167–172.
50. Takashima A, et al. Activation of tau protein kinase I/glycogen synthase kinase-3beta by amyloid beta peptide (25-35) enhances phosphorylation of tau in hippocampal neurons. *Neurosci Res*. 1998;31(4):317–323.
51. Phiel CJ, Wilson CA, Lee VM, Klein PS. GSK-3alpha regulates production of Alzheimer's disease amyloid-beta peptides. *Nature*. 2003;423(6938):435–439.
52. Jaworski T, et al. GSK-3alpha/beta kinases and amyloid production in vivo. *Nature*. 2011; 480(7376):E4–E5.
53. Alvarez G, Munoz-Montano JR, Satrustegui J, Avila J, Bogonez E, Diaz-Nido J. Lithium protects cultured neurons against beta-amyloid-induced neurodegeneration. *FEBS Lett*. 1999;453(3):260–264.
54. Qing H, et al. Valproic acid inhibits Abeta production, neuritic plaque formation, and behavioral deficits in Alzheimer's disease mouse models. *J Exp Med*. 2008;205(12):2781–2789.
55. Ray WJ, JrSzymanki ES, Ng L. The binding of lithium and of anionic metabolites to phosphoglucomutase. *Biochim Biophys Acta*. 1978;522(2):434–442.
56. Inhorn RC, Majerus PW. Inositol polyphosphate 1-phosphatase from calf brain. Purification and inhibition by Li+, Ca2+, and Mn2+. *J Biol Chem*. 1987;262(33):15946–15952.
57. Orford K, Crockett C, Jensen JP, Weissman AM, Byers SW. Serine phosphorylation-regulated ubiquitination and degradation of beta-catenin. *J Biol Chem*. 1997;272(40):24735–24738.
58. De Sarno P, Li X, Jope RS. Regulation of Akt and glycogen synthase kinase-3 beta phosphorylation by sodium valproate and lithium. *Neuropharmacology*. 2002;43(7):1158–1164.
59. Naerum L, Norskov-Lauritsen L, Olesen PH. Scaffold hopping and optimization towards libraries of glycogen synthase kinase-3 inhibitors. *Bioorg Med Chem Lett*. 2002;12(11):1525–1528.
60. Uemura K, et al. GSK3beta activity modifies the localization and function of presenilin 1. *J Biol Chem*. 2007;282(21):15823–15832.
61. Hoeflich KP, Luo J, Rubie EA, Tsao MS, Jin O, Woodgett JR. Requirement for glycogen synthase kinase-3beta in cell survival and NF-kappaB activation. *Nature*. 2000;406(6791):86–90.
62. Noble W, et al. Inhibition of glycogen synthase kinase-3 by lithium correlates with reduced tauopathy and degeneration in vivo. *Proc Natl Acad Sci U S A*. 2005;102(19):6990–6995.
63. Ly PTT, Cai F, Song W. Detection of neuritic plaques in Alzheimer's disease mouse model. *J Vis Exp*. 2011;(53).pii:2831.
64. Bromley-Brits K, Deng Y, Song W. Morris water maze test for learning and memory deficits in Alzheimer's disease model mice. *J Vis Exp*. 2011;(53).pii:2920.
65. Spittaels K, et al. Glycogen synthase kinase-3beta phosphorylates protein tau and rescues the axonopathy in the central nervous system of human four-repeat tau transgenic mice. *J Biol Chem*. 2000;275(52):41340–41349.
66. Cho JH, Johnson GV. Glycogen synthase kinase 3 beta induces caspase-cleaved tau aggregation in situ. *J Biol Chem*. 2004;279(52):54716–54723.
67. Jo J, et al. Abeta(1-42) inhibition of LTP is mediated by a signaling pathway involving caspase-3, Akt1 and GSK-3beta. *Nat Neurosci*. 2011;14(5):545–547.
68. Su Y, et al. Lithium, a common drug for bipolar disorder treatment, regulates amyloid-beta precursor protein processing. *Biochemistry*. 2004;43(22):6899–6908.
69. Walter J, et al. Phosphorylation regulates intracellular trafficking of beta-secretase. *J Biol Chem*. 2001;276(18):14634–14641.
70. von Arnim CA, et al. Demonstration of BACE (beta-secretase) phosphorylation and its interaction with GGA1 in cells by fluorescence-lifetime imaging microscopy. *J Cell Sci*. 2004;117(pt 22):5437–5445.
71. Klein PS, Melton DA. A molecular mechanism for the effect of lithium on development. *Proc Natl Acad Sci U S A*. 1996;93(16):8455–8459.

72. Chen G, Huang LD, Jiang YM, Manji HK. The mood-stabilizing agent valproate inhibits the activity of glycogen synthase kinase-3. *J Neurochem*. 1999;72(3):1327–1330.
73. Bhat R, et al. Structural insights and biological effects of glycogen synthase kinase 3-specific inhibitor AR-A014418. *J Biol Chem*. 2003;278(46):45937–45945.
74. Leroy K, Brion JP. Developmental expression and localization of glycogen synthase kinase-3beta in rat brain. *J Chem Neuroanat*. 1999;16(4):279–293.
75. Kaidanovich-Beilin O, Woodgett JR. GSK-3: Functional insights from cell biology and animal models. *Front Mol Neurosci*. 2011;4:40.
76. Akiyama H, et al. Inflammation and Alzheimer's disease. *Neurobiol Aging*. 2000;21(3):383–421.
77. Szekely CA, et al. Nonsteroidal anti-inflammatory drugs for the prevention of Alzheimer's disease: a systematic review. *Neuroepidemiology*. 2004; 23(4):159–169.
78. Eikelenboom P, van Exel E, Hoozemans JJ, Veerhuis R, Rozemuller AJ, van Gool WA. Neuroinflammation – an early event in both the history and pathogenesis of Alzheimer's disease. *Neurodegener Dis*. 2010;7(1–3):38–41.
79. Matsuoka Y, et al. Inflammatory responses to amyloidosis in a transgenic mouse model of Alzheimer's disease. *Am J Pathol*. 2001;158(4):1345–1354.
80. Wyss-Coray T. Inflammation in Alzheimer disease: driving force, bystander or beneficial response? *Nat Med*. 2006;12(9):1005–1015.
81. Amor S, Puentes F, Baker D, van der Valk P. Inflammation in neurodegenerative diseases. *Immunology*. 2010;129(2):154–169.
82. Chakrabarty P, et al. Massive gliosis induced by interleukin-6 suppresses Abeta deposition in vivo: evidence against inflammation as a driving force for amyloid deposition. *FASEB J*. 2010;24(2):548–559.
83. Chakrabarty P, Tianbai L, Herring A, Ceballos-Diaz C, Das P, Golde TE. Hippocampal expression of murine IL-4 results in exacerbation of amyloid deposition. *Mol Neurodegener*. 2012;7:36.
84. Shaftel SS, Kyrkanides S, Olschowka JA, Miller JN, Johnson RE, O'Banion MK. Sustained hippocampal IL-1 beta overexpression mediates chronic neuroinflammation and ameliorates Alzheimer plaque pathology. *J Clin Invest*. 2007; 117(6):1595–1604.
85. Boissonneault V, Filali M, Lessard M, Relton J, Wong G, Rivest S. Powerful beneficial effects of macrophage colony-stimulating factor on beta-amyloid deposition and cognitive impairment in Alzheimer's disease. *Brain*. 2009;132(pt 4):1078–1092.
86. Beurel E, Jope RS. Differential regulation of STAT family members by glycogen synthase kinase-3. *J Biol Chem*. 2008;283(32):21934–21944.
87. Beurel E, Jope RS. Lipopolysaccharide-induced interleukin-6 production is controlled by glycogen synthase kinase-3 and STAT3 in the brain. *J Neuroinflammation*. 2009;6:9.
88. Yuskaitis CJ, Jope RS. Glycogen synthase kinase-3 regulates microglial migration, inflammation, and inflammation-induced neurotoxicity. *Cell Signal*. 2009;21(2):264–273.
89. Yankner BA, Duffy LK, Kirschner DA. Neurotrophic and neurotoxic effects of amyloid beta protein: reversal by tachykinin neuropeptides. *Science*. 1990;250(4978):279–282.
90. Bourne KZ, Ferrari DC, Lange-Dohna C, Rossner S, Wood TG, Perez-Polo JR. Differential regulation of BACE1 promoter activity by nuclear factor-kappaB in neurons and glia upon exposure to beta-amyloid peptides. *J Neurosci Res*. 2007;85(6):1194–1204.
91. Buggia-Prevot V, Sevalle J, Rossner S, Checler F. NFkappaB-dependent control of BACE1 promoter transactivation by Abeta42. *J Biol Chem*. 2008;283(15):10037–10047.
92. Takada Y, Fang X, Jamaluddin MS, Boyd DD, Aggarwal BB. Genetic deletion of glycogen synthase kinase-3beta abrogates activation of IkappaBalpha kinase, JNK, Akt, and p44/p42 MAPK but potentiates apoptosis induced by tumor necrosis factor. *J Biol Chem*. 2004;279(38):39541–39554.
93. Steinbrecher KA, Wilson W. Glycogen synthase kinase 3beta functions to specify gene-specific, NF-kappaB-dependent transcription. *Mol Cell Biol*. 2005;25(19):8444–8455.
94. Polakis P. Wnt signaling and cancer. *Genes Dev*. 2000;14(15):1837–1851.
95. Harada N, et al. Intestinal polyposis in mice with a dominant stable mutation of the beta-catenin gene. *EMBO J*. 1999;18(21):5931–5942.
96. Cross DA, Culbert AA, Chalmers KA, Facci L, Skaper SD, Reith AD. Selective small-molecule inhibitors of glycogen synthase kinase-3 activity protect primary neurones from death. *J Neurochem*. 2001;77(1):94–102.
97. Coghlan MP, et al. Selective small molecule inhibitors of glycogen synthase kinase-3 modulate glycogen metabolism and gene transcription. *Chem Biol*. 2000;7(10):793–803.
98. Qing H, Zhou W, Christensen MA, Sun X, Tong Y, Song W. Degradation of BACE by the ubiquitin-proteasome pathway. *FASEB J*. 2004;18(13):1571–1573.
99. Sun X, He G, Song W. BACE2, as a novel APP theta-secretase, is not responsible for the pathogenesis of Alzheimer's disease in Down syndrome. *FASEB J*. 2006;20(9):1369–1376.
100. Gapuzan ME, Schmah O, Pollock AD, Hoffmann A, Gilmore TD. Immortalized fibroblasts from NF-kappaB RelA knockout mice show phenotypic heterogeneity and maintain increased sensitivity to tumor necrosis factor alpha after transformation by v-Ras. *Oncogene*. 2005;24(43):6574–6583.
101. Sun X, Tong Y, Qing H, Chen CH, Song W. Increased BACE1 maturation contributes to the pathogenesis of Alzheimer's disease in Down syndrome. *FASEB J*. 2006;20(9):1361–1368.
102. Wang R, Zhang M, Zhou W, Ly PT, Cai F, Song W. NF-kappaB signaling inhibits ubiquitin carboxyl-terminal hydrolase L1 gene expression. *J Neurochem*. 2011;116(6):1160–1170.
103. Sturchler-Pierrat C, et al. Two amyloid precursor protein transgenic mouse models with Alzheimer disease-like pathology. *Proc Natl Acad Sci U S A*. 1997;94(24):13287–13292.
104. Busche MA, et al. Clusters of hyperactive neurons near amyloid plaques in a mouse model of Alzheimer's disease. *Science*. 2008;321(5896):1686–1689.
105. Herzig MC, et al. Abeta is targeted to the vasculature in a mouse model of hereditary cerebral hemorrhage with amyloidosis. *Nat Neurosci*. 2004; 7(9):954–960.